https://doi.org/10.5194/acp-2020-100
Preprint. Discussion started: 26 February 2020

Atmospheric Chemistry and Physics Discussions

Temperature and VOC concentration as controlling factors for chemical composition of alpha-pinene derived secondary organic aerosol

Louise N. Jensen[1], Manjula R. Canagaratna[2], Kasper Kristensen[3], Lauriane L. J. Quéléver[4], Bernadette Rosati[1,5], Ricky Teiwes[5], Marianne Glasius[1], Henrik B. Pedersen[5], Mikael Ehn[4], Merete Bilde[1]

[1]Department of Chemistry, Aarhus University, 8000 Aarhus C, Denmark
[2]Aerodyne Research, Inc., Billerica, MA, USA
[3]Department of Engineering, Aarhus University, 8000 Aarhus C, Denmark
[4]Institute for Atmospheric and Earth System Research – INAR / Physics, P.O. Box 64, FI-00014, University of Helsinki, Finland
[5]Department of Physics and Astronomy, Aarhus University, 8000 Aarhus C, Denmark

Correspondence to: Merete Bilde (bilde@chem.au.dk)

Abstract

This work investigates the individual and combined effects of temperature and volatile organic compound precursor concentration on the chemical composition of particles formed in the dark ozonolysis of α-pinene. All experiments were conducted in a 5 m^3 Teflon chamber at an initial ozone concentration of 100 ppb and α-pinene concentrations of 10 ppb and 50 ppb, respectively, at constant temperatures of 20 °C, 0 °C, or -15 °C, and at changing temperatures (ramps) from -15 °C to 20 °C and from 20 °C to -15 °C. The chemical composition of the particles was probed using a High-Resolution Time-of-Flight Aerosol Mass Spectrometer (HR-ToF-AMS).

A four-factor solution of a Positive Matrix Factorization (PMF) analysis of combined HR-ToF-AMS data from experiments conducted under different conditions is presented. The PMF analysis as well as elemental composition analysis of individual experiments show that secondary organic aerosol particles with the highest oxidation level are formed from the lowest initial α-pinene concentration (10 ppb) and at the highest temperature (20 °C). Higher initial α-pinene concentration (50 ppb) and/or lower temperature (0 °C or -15 °C) result in lower oxidation level of the molecules contained in the particles. With respect to carbon oxidation state, particles formed at 0 °C are more comparable to particles formed at -15 °C than to those formed at 20 °C. A remarkable observation is that changes in temperature during or after particle formation result in only minor changes in the elemental composition of the particles. The temperature at which aerosol particle formation is initiated thus seems to be a critical parameter for the particle elemental composition.

Comparison of the AMS derived estimates of the content of organic acids in the particles based on m/z 44 in the spectra show good agreement with results from off-line molecular analysis of particle filter samples collected from the same experiments. While higher temperatures are associated with a decrease in the absolute mass concentrations of organic acids (R-COOH) and organic acid functionalities (-COOH), the organic acid functionalities account for an increasing fraction of the measured SOA mass at higher temperatures.

https://doi.org/10.5194/acp-2020-100
Preprint. Discussion started: 26 February 2020

Atmospheric Chemistry and Physics Discussions

1 Introduction

Atmospheric aerosol particles can alter air quality (WHO 2016) and visibility (Wang et al. 2009) on a regional scale. On a global scale, particles affect cloud formation, the radiative balance, and thus climate (IPCC 2013).

Atmospheric particles are chemically diverse entities, often with a significant mass fraction of organic compounds (Zhang et al. 2007; Jimenez et al. 2009). Secondary Organic Aerosol (SOA) is formed from condensation of oxidation products of volatile organic compounds (VOC) emitted from both anthropogenic and biogenic sources (Guenther et al. 1995; Sindelarova et al. 2014). α-pinene is a biogenic VOC emitted from e.g. foliage of coniferous trees (Rasmussen 1972), and has it been identified as the most common monoterpene in boreal forest all year round (Hakola et al. 2003). In the atmosphere, α-pinene is oxidized primarily by ozone (O_3), hydroxyl radicals (OH^-), and nitrate radicals (NO_3^-). Due to their low vapor pressures, some of the gas phase oxidation products may partition onto already existing particles and contribute to particle growth (Hallquist et al. 2009). In addition, some low vapor pressure oxidation products of α-pinene are able to nucleate (Kirkby et al. 2016) and are likely to play an important role in the initial growth of new particles in the atmosphere (O'Dowd et al. 2002; Riipinen et al. 2012; Ehn et al. 2014; Tröstl et al. 2016).

It is well established that the particle mass available for condensation of gases affects the partitioning of organic species between gas phase and particle phase (Pankow 1994a, 1994b), although the traditional partitioning theory is limited in relation to non-liquid, more viscous particles e.g. α-pinene derived SOA formed at low relative humidity (Renbaum-Wolff et al. 2013), because of slow diffusion (Cappa and Wilson, 2011; Pöschl, 2011).

The fraction (F) of a given semi-volatile species in the particle phase at a given temperature has been formulated in an absorptive equilibrium partitioning framework as

$$F = \frac{1}{1 + c^*/M} \qquad (1)$$

where c* is the gas phase mass concentration at saturation and M is the mass concentration of absorbing material (Kroll and Seinfeld 2008). Thus, the chemical composition of a particle that is in equilibrium with the surrounding gas phase is affected by both c* and M. The c* of a gaseous compound is generally inversely related to its level of oxidation (Jimenez et al. 2009). The particle composition can be shifted towards species with higher c* values (i.e. less oxidized species) by increasing the mass concentration of pre-existing particles, i.e. the value of M; conversely, lower M values result in particle phase compositions that are dominated by species with lower c* values (i.e. more oxidized species). This has been experimentally confirmed by e.g. Shilling et al., (2009) who showed that the oxidation level of SOA from α-pinene ozonolysis decreases with increasing particle mass loadings.

The volatility of gases (c*) also depends on temperature, which affects equilibrium partitioning and thereby particle mass as demonstrated by Pathak et al. (2007), Saathoff et al. (2009), and Warren et al. (2009) based on chamber studies of α-pinene derived particles formed at different constant temperatures between -30 °C and 45 °C. Partitioning has also been addressed in chamber studies where the temperature was changed after the initial formation of SOA. Stanier et al. (2007) increased the temperature from 22 °C to a maximum of 40 °C and in some experiments decreased the temperature back again to 22 °C. During heating, they observed a decrease in SOA size and during cooling an increase in SOA size. In experiments by Warren et al. (2009), where the temperature was cycled in the ranges of 5 °C to 27 °C and 27 °C to 45 °C, heating was associated with a decrease in particle mass and cooling associated with an increase in particle mass.

The chemical composition of gas and particle phase in α-pinene ozonolysis experiments is determined by a combination of thermodynamic and kinetic aspects (Zhang et al. 2015; Kristensen et al. 2017). The effect of temperatures below room temperature (around 20 °C), in particular below 0 °C, on gas phase oxidation products, nucleation, SOA growth, and particle chemical composition, however, remains a largely unexplored area. Since low temperatures are of high atmospheric relevance

https://doi.org/10.5194/acp-2020-100
Preprint. Discussion started: 26 February 2020

Atmospheric Chemistry and Physics Discussions

due to their prevalence, e.g. at the latitudes of the boreal forests and at higher elevation, it is important to quantify SOA formation and properties under cold conditions. Furthermore, vertical transport can lead to changes in temperature within short time frames affecting reaction kinetics, condensation processes, and particle properties relevant for climate (Topping et al. 2013; Murphy et al. 2015).

The lack of knowledge on how the chemical composition, of both the gas phase and particle phase, vary with temperatures was the motivation behind the Aarhus Chamber Campaign on HOMs and Aerosols (ACCHA) introduced in the companion paper Kristensen et al. (manuscript submitted). The impact of temperature on highly oxygenated organic molecules (HOMs) yield is presented in Quéléver et al. (2019) and more details on the volatile organic compounds are presented in Rosati et al. (2019).

The goal of the current paper is to investigate and quantify the individual and combined effects of α-pinene precursor concentration and temperature on SOA mass concentration and chemical composition. For this purpose we here describe and discuss a subset of the data collected during the ACCHA campaign focusing on results obtained from a High-Resolution Time-of-Flight Aerosol Mass Spectrometer (HR-ToF-AMS).

2 Methods

2.1 Experimental

This work is based on experiments conducted in the Aarhus University Research on Aerosol (AURA) chamber; a ~5 m^3 bag made of 125 µm FEP Teflon film located in an enclosure where the temperature is controllable between -16 °C and 26 °C. The AURA chamber has been described in detail by Kristensen et al. (2017).

The experiments were conducted as part of the ACCHA campaign and focus on dark ozonolysis of α-pinene. An overview of the campaign is provided in Kristensen et al. (manuscript submitted). To ease the reading of the current paper a short summary of the ACCHA campaign is given here and an experimental overview table with focus on the parameters relevant in this work is presented (Table 1). At a constant chamber temperature of either 20 °C, 0 °C, or -15 °C, ozone was injected into the chamber to a concentration of ~100 ppb followed by injection of either 10 ppb α-pinene (low concentration) or 50 ppb α-pinene (high concentration). The chamber was operated at atmospheric pressure and neither seed particles nor OH-scavengers were introduced.

Three series of constant temperature experiments, all consisting of an experiment at 20 °C, 0 °C, and -15 °C, were conducted. One of the series was performed at the initial α-pinene concentration of 10 ppb (experiments 1.1-1.3), and two series of experiments were initiated at 50 ppb α-pinene (experiments 2.1-2.3 and 3.1-3.3). 220-272 minutes after α-pinene injection (i.e. after the SOA mass concentration has peaked) in the series consisting of experiments 2.1-2.3, the temperature was in a continuous ramp changed from the original setting, either by cooling the chamber from 20 °C to -15 °C (experiment 2.1), by cooling from 0 °C to -15 °C followed by heating to 20 °C (experiment 2.2), or by heating from -15 °C to 20 °C (experiment 2.3). In two additional experiments with an initial α-pinene concentration of 10 ppb (experiments 1.4 and 1.5) the temperature was ramped from the initial temperature at 20 °C to -15 °C and from -15 °C to 20 °C, respectively, ~35 minutes after α-pinene injection (i.e. during formation and before the peak in SOA mass concentration).

In this work, we present data from a subset of instruments involved in the ACCHA campaign: a temperature and humidity sensor (HC02-04) attached to a HygroFlex HF320 transmitter (Rotronic AG) placed in the center of the chamber, a scanning mobility particle sizer (SMPS) consisting of a Differential Mobility Analyzer (DMA, TSI 3082) and a nano water-based condensation particle counter (CPC, TSI 3788), and a High-Resolution Time-of-Flight Aerosol Mass Spectrometer (HR-ToF-AMS, Aerodyne Research Inc.) (Jayne et al. 2000; DeCarlo et al. 2006; Canagaratna et al. 2007). In the following, the HR-

https://doi.org/10.5194/acp-2020-100
Preprint. Discussion started: 26 February 2020

Atmospheric Chemistry and Physics Discussions

ToF-AMS will be referred to as AMS. Both the SMPS and AMS were placed at room temperature next to the chamber outlets and the connecting tubing was temperature insulated.

By the end of each experiment, a particle sample was collected on a Teflon filter (0.45 µm pore size, Chromafil). Particle samples were extracted and analyzed by an Ultra High Performance Liquid Chromatograph/Electrospray Ionization quadrupole Time-of-Flight Mass Spectrometer (UHPLC/ESI-qTOF-MS, Bruker Daltonic) as described in Kristensen et al. (manuscript submitted), where also the analytical method and results are presented in detail. Herein we compare the findings from the UHPLC/ESI-qTOF-MS, hereafter referred to as LC-MS, and the AMS measurements.

2.2 Data analysis

Positive Matrix Factorization (PMF) (Paatero and Tapper 1994; Paatero 1997) has traditionally been used to investigate contributions of different sources to ambient particles and the application of PMF to AMS data from chamber experiments was first demonstrated by Craven et al. (2012). In the present work, PMF analysis is applied to chemical composition data from SOA particles that are produced in the ozonolysis of α-pinene but formed and aged under different temperatures and precursor concentrations and consequently different particle loadings. AMS mass spectra of SOA particles from the various experimental conditions were analyzed in one matrix, allowing for monitoring spectral and elemental chemical composition changes that occur as conditions change. The PET tool (V 2.09A) was used to perform the PMF analysis on high resolution AMS mass spectra according to the principles described in detail by Ulbrich et al. (2009).

PMF is a model that can be used to express measured mass spectra as a linear combination of factors that are the products of constant mass spectra and related time profiles as follows:

$$x_{ij} = \sum_{p} g_{ip} f_{pj} + e_{ij} \qquad (2)$$

The measured mass spectral data is the matrix X, an $m \times n$ matrix with n ion masses measured at m different time points, and x_{ij} is an element of this matrix. p is the number of factors chosen for the solution, g_{ip} is an element of the matrix G containing time series of the factors, and f_{pj} is an element of the matrix F of constant factor mass spectral profiles. The matrix elements e_{ij} correspond to the error matrix, E, of residuals not explained by the model (Paatero 1997; Ulbrich et al. 2009). Equation (2) is solved using the PMF2 algorithm (Paatero 1997) which uses linear least-squares fitting together with the constraints that the values of matrix F and G have to be non-negative. The solution is found by minimizing the fit parameter Q:

$$Q = \sum_{i=1}^{m} \sum_{j=1}^{n} \left(\frac{e_{ij}}{\sigma_{ij}} \right)^2 \qquad (3)$$

where σ_{ij} is an element of a matrix containing the standard deviations for each element of X (Paatero 1997; Ulbrich et al. 2009). Estimation of standard deviations was performed as outlined in Ulbrich et al. (2009) with "weak" ions (i.e. ions with signal/noise (S/N) < 2) being down weighted by a factor of two and "bad" ions (i.e. ions with S/N < 0.2) being down weighted by a factor of ten. The number of factors (p) are chosen based on a combination of evaluation of residuals, Q values, and a priori knowledge about the dataset (Lanz et al. 2007; Ulbrich et al. 2009). In the result section, a four-factor solution of the PMF analysis of AMS HR data is presented. Although the five and six factor solutions have lower $Q/Q_{expected}$ ($Q_{expected} \approx m \times n$, i.e. the number of points in the data matrix (Ulbrich et al. 2009)) compared to the four-factor solution, the higher number of

https://doi.org/10.5194/acp-2020-100
Preprint. Discussion started: 26 February 2020

Atmospheric Chemistry and Physics Discussions

factors does not provide additional information. Plots of the $Q/Q_{expected}$ and the residuals of the four, five, and six factor solutions, as well as the results of the five and six factor solutions are shown in the supplementary material (S1-S8).

Since previous laboratory experiments show that the collection efficiency (CE) and relative ionization efficiency (RIE) of laboratory SOA is variable (Docherty et al. 2013), the mass concentrations presented in the PMF analyses are estimated from the total SOA mass concentration as obtained from integrated SMPS size distributions assuming spherical particles and densities calculated from the AMS-derived elemental ratios (Kuwata et al. 2011). Densities are derived as averages based on AMS data from the last 30 minutes of each experiment, except for experiments 2.1-2.3 where only the part of the experiment where the temperature is kept constant is included.

3 Results and discussion

To provide an overview of the course of a typical experiment, Figure 1a shows the evolution in particle mass concentration, density, and the elemental composition illustrated by the oxygen-to-carbon (O:C) ratio in experiment 2.3, conducted at -15 °C and with an initial α-pinene concentration of 50 ppb. Initially both the density and O:C ratio increase significantly but from ~50 minutes onwards the O:C ratio stabilizes and only slightly increases while the density slightly decreases. After ~175 minutes the particle mass peaks (not corrected for wall loss). Under all conditions (i.e. in all experiments), the AMS derived SOA densities are in the range 1.1 to 1.3 g cm^{-3}. Figure S9 however reveals a slight increase in density with higher particle formation and aging temperature, and a slightly higher density for the particles formed at low α-pinene concentration compared to high α-pinene concentration.

Figure 1b is a mass spectrum of Experiment 2.3 obtained from the high resolution AMS data at the highest particle mass concentration (not wall loss corrected). It shows that fragments which belong to the so-called hydrocarbon family (CH) are distributed throughout the mass spectrum, with some of the most prominent peaks (and ions) being m/z 39 ($C_3H_3^+$), 41 ($C_3H_5^+$) and 55 ($C_4H_7^+$). The oxidized compounds, which belong to the CHO and CHOgt1 (gt means greater than) families, dominate at m/z 28 (estimated from CO_2^+ according to Aiken et al. (2008)), 29 (CHO^+), 43 ($C_2H_3O^+$), 44 ($C_2H_4O^+$, CO_2^+), 55 ($C_3H_3O^+$), and 83 ($C_5H_7O^+$). m/z 43 is the most significant peak and has the highest contribution of the CHO family, while the CHOgt1 family dominates in m/z 44. Previous studies have shown that these two peaks provide useful information about particle oxidation level (Ng et al. 2011). The patterns described above are also observed in the mass spectra of the other experiments and overall the mass spectra are highly comparable across experimental conditions (Supplementary material S10-S20) as well as to mass spectra of particles formed in the α-pinene ozonolysis in other chambers (Bahreini et al. 2005; Song et al. 2007; Shilling et al. 2009; Chhabra et al. 2010).

3.1 PMF analysis of Aerosol Mass Spectra

While PMF is traditionally utilized to identify distinct sources in ambient measurements, here PMF analysis of a combined dataset of α-pinene SOA experiments provides a tool for identifying subtle changes in the measured mass spectra across the different experimental conditions. The analysis was performed on a combined dataset representing eight different experimental conditions: three constant temperatures, 20 °C, 0 °C, and -15 °C, at two α-pinene concentrations, 10 and 50 ppb (experiments 1.1, 1.2, 1.3, 3.1, 3.2, and 3.3) and two temperature ramps, from 20 °C to -15 °C and from -15 °C to 20 °C, both at an α-pinene concentration of 10 ppb (experiments 1.4 and 1.5).

The result of the four-factor solution from the PMF analysis is presented in Figure 2, showing the changes in mass concentration of the factors as a function of time in each experiment, and in Figure 3, showing the high-resolution mass spectra of the four factors, i.e. factor profiles. As expected from the comparison of the mass spectra from the individual experiments (Supplementary material S10-S20), the factor profiles (Figure 3) show a high degree of similarity with small differences in the relative intensities of ions.

https://doi.org/10.5194/acp-2020-100
Preprint. Discussion started: 26 February 2020

Atmospheric Chemistry and Physics Discussions

As shown in Figure 2, the relative contributions of the different factors to the observed SOA particle mass concentration vary across different temperatures and α-pinene concentrations (i.e. particle mass loadings). At high temperature, Factor 1 dominates whereas Factor 4 is less significant, while at low temperature Factor 4 dominates and Factor 1 is less significant. Correspondingly, at high α-pinene concentration, Factor 2 dominates and Factor 3 is less significant while the opposite is the case at low precursor concentration. This means, that the profiles of the factors represent characteristics of the particle chemical composition associated with temperature and precursor concentration.

According to their appearance Factors 1 and 4 will in the following discussion be referred to as temperature factors and Factors 2 and 3 will be referred to as concentration factors. For each factor, Table 2 provides the oxygen-to-carbon (O:C) ratio, hydrogen-to-carbon (H:C) ratio, as well as the ratio between the absolute intensities of the fragment ions at m/z 43 ($C_3H_7^+$, $C_2H_3O^+$) and the total organic ion intensity (f_{43}), and the ratio between the absolute intensities of the fragment ions at m/z 44 ($C_2H_4O^+$, CO_2^+) and the total organic ion intensity (f_{44}).

Figure 3 shows the mass spectrum colored according to contributions from the various types of elemental compositions (i.e. ion families) that appear at each ion signal. Factor 1 (high temperature) is the factor that is mostly dominated by ions from oxidized species (i.e. high intensity of CHO and CHOgt1 ion groups at m/z 28, 29, 43, 44, 55, and 83). In Factor 1, the intensity of the ions at m/z > 44 is in general low in comparison with the other factors. Among all factors, Factor 1 has the highest O:C ratio (0.56), f_{43} (14 %), and f_{44} (9 %) and therefore the chemical species represented by Factor 1 are likely the most oxidized and least volatile of all those present in the SOA. Factor 4 (low temperature) has around the same level of f_{43}, (13 %) as Factor 1 and relative high intensities of m/z 55 and m/z 83, which are the fragment ions larger than m/z 43 that are most intense in the CHO1 ion family. On the other hand, Factor 4 is low in the more oxidized f_{44} (4 %) and consequently the O:C ratio (0.34) is much lower compared to Factor 1 (high temperature).

Factor 3 (low α-pinene concentration) has the second highest contribution of oxidized ions (CHO1 and CHOgt1 family), O:C ratio (0.39), and f_{44} (8 %). With an f_{43} (7 %) being of similar magnitudes as f_{44}, it also has the highest relative ratio of f_{44}-to-f_{43} among the four factors. Furthermore, Factor 3 also has strong contributions from hydrocarbons (CH family) such as m/z 39, 41, 55, 67, 69, 79, 81, and 91. For comparison, Factor 2 (high α-pinene concentration) has a slightly lower f_{43} (10 %) (Factor 2) and the lowest f_{44} (3 %) and O:C (0.26) among all factors, i.e., it represents the least oxidized material. It is noticed that Factor 2 has relative high contributions from the CHO1 family at m/z 55 and m/z 83 and among all factors, it has the highest contribution of m/z 91 from the CH family, which has been used as a tracer of biogenic emissions in ambient measurements (Lee et al. 2016).

Overall, the factors related to temperature variation (Factors 1 and Factor 4) show a larger difference in oxidation level than the factors related to α-pinene concentration, i.e. particle mass loading (Factors 2 and 3). This suggests that within the investigated conditions, differences in temperature (20 °C to -15 °C) have a larger effect on particle chemical composition than VOC concentration (10 and 50 ppb α-pinene).

It is interesting to notice that the O:C and H:C ratios of Factor 1 (high temperature) and Factor 3 (low concentration) are similar to results presented by Lee et al. (2016) who used PMF analysis to explore the SOA sources in a coniferous forest mountain region in British Columbia. PMF factors obtained from the ambient AMS data showed a background source and two biogenic SOA sources: BSOA1 from terpene oxidized by ozone and nitrate radical during nighttime, and BSOA2 from terpene oxidized by ozone and OH-radical during daytime. Overall, the mass spectrum of BSOA1 from Lee et al. (2016) is highly comparable to the spectra obtained in these experiments. In the BSOA1 factor, the O:C ratio is 0.56 and the H:C ratio 1.56. These levels have a high similarity with Factor 1 (high temperature) and Factor 3 (low concentration), consistent with the fact that in the ambient measurements by Lee et al., (2016), SOA concentrations reached up to 5 μg m^{-3} and the temperature varied from ~5 °C to ~25 °C, corresponding to the SOA mass level in the low α-pinene concentration experiments (Figure 2) and the temperature in the upper range of the experiments presented in this paper. The good agreement between PMF factors from

https://doi.org/10.5194/acp-2020-100
Preprint. Discussion started: 26 February 2020

Atmospheric Chemistry and Physics Discussions

laboratory and ambient observations indicates that the PMF analysis of chamber SOA chemical composition obtained under different temperature and loading conditions can be useful for the interpretation and understanding of ambient SOA composition and vice versa.

3.2 Trends in chemical composition

3.2.1 Elemental analysis

Studying the evolution of the elemental composition of SOA can provide insight into the chemical changes occurring during chemical and physical processes. Van Krevelen plots (Van Krevelen 1950) of the H:C ratios and O:C ratios derived from the AMS data (Aiken et al. 2007; Aiken et al. 2008; Canagaratna et al. 2015) in the constant temperature experiments (1.1-1.3, 2.1-2.3, and 3.1-3.3) are shown in Figure 4. The slight differences between the 50 ppb α-pinene experiments conducted at similar temperature might be a result of experimental uncertainty. The figure reveals interesting tendencies, both in relation to elemental composition at particle mass peak (Figure 4a) and to time evolution (Figure 4b). The Van Krevelen plots show that the SOA consists of less oxidized compounds in experiments conducted at low temperature and high α-pinene concentration, compared to high temperature and low α-pinene concentration. This trend is in agreement with the observations from the PMF analysis and with previous work (Shilling et al. 2009). For comparison the O:C ratio and H:C ratio of the four factors from the PMF analysis of the combined experimental dataset (Figures 2 and 3), are also shown in Figures 4a and 4b. The O:C and H:C ratios of the factors encompass the data from the individual experiments, illustrating how the factors from the PMF analysis captures and defines the extremes in the diversity in chemical composition in particles from the individual experiments as a result of different experimental conditions. The largest differences in elemental ratios are observed between the SOA produced under different temperatures.

Although ageing of oxidized organic particles in ambient measurements is associated with an increase in O:C ratio (Ng et al. 2011), in laboratory experiments at higher particle mass concentrations, the O:C ratio is usually observed to decrease during particle aging (Shilling et al. 2009; Chhabra et al. 2010; Denjean et al. 2015b) because of increased partitioning of less oxidized semi volatile compounds into the particle phase. Figure 4b shows that during all constant temperature 10 ppb α-pinene experiments the O:C ratio and the H:C ratio are almost constant.

Interestingly, in the 50 ppb α-pinene experiments conducted at lower temperatures (0 °C and -15 °C, experiment 2.2, 2.3, 3.2, and 3.3) the H:C and O:C ratios are simultaneously increasing during the experiment. This is not a commonly reported trend, neither in ambient measurements (Ng et al. 2011; Lee et al. 2016) nor in chamber experiments focusing on α-pinene derived SOA (Chhabra et al. 2011). Several mechanisms could potentially explain the observed evolution of SOA elemental composition in the Van Krevelen plot, and in fact, it could be due to a combination of different simultaneous mechanisms, e.g. oxidation and oligomerization. Since no OH scavenger is added in our experiments one explanation could be related to OH chemistry; Qi et al. (2012) demonstrated that exposure of α-pinene SOA formed by ozonolysis to OH-radicals increased the O:C ratio, and also lead to higher H:C ratio because of OH addition to the unsaturated VOC. Modelling suggests, however, that the OH oxidation is not more pronounced at low temperature (0 °C) compared to high temperature (20 °C) (Quéléver et al., 2019), which makes this a less likely explanation for the continuous increase in the O:C ratio and H:C ratio in the cold experiments. While the simultaneous increase in H:C ratio and O:C ratio could also be associated with hydration reactions (Heald et al. 2010) with carbonyls (Axson et al. 2010), condensation of water does not influence the elemental ratios derived from the AMS spectra since the calculation does not directly utilize measured H_2O-related ion signals as they typically have large interferences from gas phase H_2O in air (Canagaratna et al. 2015). It should be mentioned, that the observed increase in H:C ratio could potentially be due to impurities condensing to the particle phase in the cold experiments although this seems highly unlikely, as the chamber was cleaned thoroughly before the experiments (see Kristensen et al., manuscript submitted),

https://doi.org/10.5194/acp-2020-100
Preprint. Discussion started: 26 February 2020

Atmospheric Chemistry and Physics Discussions

and the changes in H:C ratios would need an excessive amount of impurities as the particle mass is high (see Table 1, and Figure 2). Finally, since the increase in H:C ratio is only observed in the cold experiments, it is possible that the H:C ratios for the chamber SOA species that condense at the lower temperatures are less accurate, because these species are not well represented in the calibration dataset that was used to formulate the method (Canagaratna et al. 2015) by which the H:C ratio (and O:C ratio) is derived from AMS spectra.

Figure 5 illustrates the evolution in the O:C ratio during temperature ramps and constant temperature experiments. The time series of the O:C ratio in the 10 ppb α-pinene experiments (1.1-1.5) and the 50 ppb α-pinene experiments (2.1-2.3 and 3.1-3.3) are shown in Figures 5a and 5b respectively. In the 10 ppb α-pinene experiment (1.4) where the temperature is cooled 36 minutes after experimental start, the temperature change from 20 °C to -15 °C is associated with a decrease in the O:C ratio, which corresponds to condensation of less oxidized, i.e. more volatile, species (Figure 5a). Conversely, heating the particles from -15 °C to 20 °C 34 minutes after experimental start (experiment 1.5) results in an increase of O:C as more volatile, less oxidized species evaporate and increase the O:C ratio of the remaining particle mass. For comparison, Denjean et al. (2015a) also observed a slight increase in O:C ratio when increasing the temperature by 6 °C in the room temperature range. In relation to the 50 ppb α-pinene experiments where temperature is changed 220-272 minutes after experimental start (Figure 5b), the same trend in O:C ratio is observed, but interestingly the increase in the O:C ratio in these heating ramp experiments does not start immediately.

An important outcome of Figure 5 is that the O:C ratios at the end of the ramps are closer to the O:C ratios of the particles in the experiments conducted at the temperature where the ramps start than where they end. This observation suggests that the composition of α-pinene-derived particles is, to a large extent, controlled by the temperature at which they are initially formed and that subsequent changes in temperature, even as dramatic as 35 °C during 100-130 minutes, do not change the particle chemical composition significantly. Even though the newly formed particles are exposed to this change in temperature (~35 minutes after experimental start, and ~1 hour before SOA mass peak (Figure 2)), only slight changes in the chemical composition are observed (Figure 5a).

3.2.2 Oxidized organic tracer ions

As described in relation to the mass spectra obtained from the PMF analysis (Figure 3), differences in VOC precursor concentration (i.e., particle mass loading) and temperature primarily result in intensity differences in the dominant oxygen-containing ions, m/z 43 and m/z 44. m/z 43 (dominated by $C_2H_3O^+$ (CHO family)) likely derives from organic compounds containing non-acid oxygen (Ng et al. 2010), while the signal at m/z 44 (primary CO_2^+ (CHOgt1 family)) arises from carboxylic acids (Alfarra 2004). Both the number of acid groups and the length and functionalization of the carbon chain in the compounds affect the intensity of the signal at m/z 44 (Alfarra et al. 2004; Canagaratna et al. 2015).

Figures 6a and 6b are “triangle plots” (Ng et al. 2010) showing f_{44} (the fraction of m/z 44 relative to the total mass in the spectra) as a function of f_{43} (the fraction of m/z 43 relative to the total mass in the spectra) obtained from unit mass resolution data from the AMS. Figure 6a shows the values at the peak of mass concentration (five data point average) of constant temperature experiments (1.1-1.3, 2.1-2.3, and 3.1-3.3) and temperature ramp experiments (1.4 and 1.5) while Figure 6b shows the evolution through the constant temperature experiments. As observed in the Van Krevelen plots (Figures 5a and 5b), data from the repeated 50 ppb α-pinene experiments (2.1-2.3 and 3.1-3.3,) conducted at similar temperatures show good reproducibility, though not being identical.

The triangle plots show that particles formed at higher temperature have a higher f_{44} (i.e. CO_2^+, acid-derived functionalities) than particles formed at lower temperature. No clear tendencies with temperature are observed for f_{43} (i.e. $C_2H_3O^+$, non-acid-derived functionalities). Particles formed at lower α-pinene concentration (10 ppb) have higher f_{44} and a lower f_{43} than particles formed at higher α-pinene concentration (50 ppb). This suggests that acid-derived functionalities are more prevalent in α-

https://doi.org/10.5194/acp-2020-100
Preprint. Discussion started: 26 February 2020

Atmospheric Chemistry and Physics Discussions

pinene SOA formed at low precursor concentration. In all experiments, f_{44} values are between 0.04 and 0.1 and f_{43} values are between 0.08 and 0.15. These are comparable to values reported in the literature from chamber experiments conducted at comparable α-pinene concentrations, both at room temperature (Chhabra et al. 2011; Kristensen et al. 2017) and at -15 °C (Kristensen et al. 2017). The continuous increase in f_{43} (Figure 6b) in the experiments conducted at -15 °C (experiments 1.3, 2.3, and 3.3) and to some extent at 0 °C (experiments 1.2, 2.2, and 2.3), are in agreement with observations by Kristensen et al. (2017) from experiments performed at -15 °C at identical α-pinene concentration. Moreover, the non-evolving f_{43} at 20 °C is also in agreement with literature exploring α-pinene SOA at comparable concentrations and room temperature (Chhabra et al. 2011; Kristensen et al. 2017). As the increase in f_{43} is only observed in the cold experiments, especially -15 °C, this suggests that formation of species that give rise to high f_{43} values are highly temperature dependent.

3.2.3 Estimated particle content of organic acids

In AMS mass spectra, m/z 44 has been shown to be a good tracer for the content of organic acids in SOA (Canagaratna et al. 2015; Yatavelli et al. 2015). Yatavelli et al. (2015) investigated how the mass of molecules (R-COOH) containing one or more acid functionalities can be related to the AMS derived mass of m/z 44 multiplied by scaling factors. In this work Yatavelli et al. (2015) estimated that 10 to 50 % of the organic particle mass in the northern hemisphere can be attributed to molecules containing the carboxylic acid functionality. Inspired by Yatavelli et al. (2015) we here explore how the intensity of m/z 44 in the AMS mass spectra compares to the mass of organic acids (R-COOH) and organic acid functionalities (-COOH) obtained by the off-line LC-MS results from the AURA chamber experiments. As described in detail in Kristensen et al. (manuscript submitted) LC-MS analysis was performed to identify and quantify the 10 carboxylic acids which are regarded as some of the most important in α-pinene derived SOA and in current experiments constitute 18-38 % of the SOA mass, as well as 30 dimer esters which together constitute 4-11 % of the total SOA mass.

For the 50 ppb α-pinene experiments 3.1, 3.2, and 3.3, conducted at 20 °C, 0 °C, and -15 °C, respectively, Figure 7a shows the mass concentration of organic acids (R-COOH) identified from LC-MS analysis (Kristensen et al., manuscript submitted) and the mass concentration of the m/z 44 signal in the AMS mass spectra, scaled to the SMPS mass and corrected for density as previously described. For both techniques the mass concentration of organic acids is lower at higher temperatures. The AMS m/z 44 mass concentrations are lower than the organic acid concentrations obtained from the LC-MS by factors of 2.55, 4.11, and 4.65 at 20 °C, 0 °C, and -15 °C, respectively. For comparison, Yatavelli et al. (2015) reported the m/z 44 AMS signal being a factor of ~2.32 lower than the mass concentration of organic acids in SOA during summertime in a forest area dominated by pine trees near Colorado Springs, USA. Their result is in very good agreement with the scaling factor obtained in the experiment conducted at 20 °C, which supports the hypothesis that the most important organic acids in pinene SOA are determined by the LC-MS method. The variation in scaling factors at the different temperatures likely reflects that organic acids with different numbers of acid functionality (-COOH) and/or different multifunctional moieties exhibit different degrees of thermal decomposition to the m/z 44 signal in the AMS (Canagaratna et al. 2015; Yatavelli et al. 2015). The similarity of the scaling factors obtained in the 0 °C (4.11) and -15 °C (4.65) experiments is consistent with the fact that the SOA chemical composition at those temperatures have a higher degree of comparability relative to the 20 °C experiment where a lower scaling factor (2.55) is obtained (recall Figures 4 and 6).

Since lower SOA mass is produced at the higher temperatures, it is also relevant to investigate how the mass fractions of organic acids vary with temperature (Figure 7b). The mass fractions are obtained by dividing the LC-MS and AMS results presented in Figure 7a by the total SOA mass concentration measured in the chamber, prior to the filter sampling, and corrected as described previously. By application of the scaling factors found above, the two techniques are in good agreement, though slight differences appears at 20 °C and -15 °C. While the mass of organic acids (R-COOH) obtained from the LC-MS decreased significantly with higher temperature (Figure 7a), no trend is observed in organic acid mass fractions (Figure 7b). Interestingly,

https://doi.org/10.5194/acp-2020-100
Preprint. Discussion started: 26 February 2020

Atmospheric Chemistry and Physics Discussions

for m/z 44 from the AMS mass spectra, the temperature dependent trend changes from decreasing with higher temperature (Figure 7a) to increasing when focusing at the mass fraction of m/z 44 to total SOA mass (Figure 7b).

Some of the organic acids as well as the dimers observed from the LC-MS data (Figures 7a and 7b) contain multiple acid functionalities (-COOH) (Kristensen et al., manuscript submitted). Therefore it is also relevant to investigate how the mass and mass fraction of acid functionalities from the suggested molecular structures (Kristensen et al., manuscript submitted) relate to the m/z 44 signal obtained from the AMS. Lower masses of organic acid functionalities (-COOH) are obtained at higher temperatures, and the scaling factors of 1.15, 1.46, and 1.70 applied to the m/z 44 AMS signal at 20 °C, 0 °C, and -15 °C, respectively (Figure 7c), are lower and less variable with temperature than those for the mass of organic acids (R-COOH, Figure 7a). The difference between the scaling factors related to the mass of organic acids (R-COOH, Figure 7a) and organic acid functionalities (-COOH, Figure 7c) at the same temperatures reflects the mass of the organic acid backbone (i.e. R in R-COOH). The observed trends in Figures 7a and 7c suggest that organic acids with heavier backbones are formed at temperatures below 20 °C.

Figure 7d shows that carboxylic acid functionalities (-COOH) account for a greater fraction of the observed SOA mass at higher temperatures, consistent with the observation of higher f_{44} values at higher temperatures in Figure 6. This trend is opposite from the temperature dependent trend of the absolute mass of organic acid functionalities (-COOH, Figure 7c) and organic acids (R-COOH, Figure 7b) also found in previous studies (Zhang et al. 2015; Kristensen et al. 2017).

Overall, the comparison of the m/z 44 signal from the AMS mass spectra and SOA acid content obtained from LC-MS data shows that organic acids and organic acid functionalities are important constituents of α-pinene derived SOA and that it is relevant to investigate and compare different techniques for their quantification.

4 Conclusion

Chemical composition of α-pinene derived SOA was investigated using HR-ToF-AMS in a series of experiments performed at different α-pinene concentrations (10 ppb and 50 ppb) and temperatures (20, 0, and -15 °C respectively). PMF analysis was applied to a combined AMS dataset representing all of these conditions. The PMF analysis revealed that the chemical composition of the SOA particles could be described by four factors which differ in their dependence on VOC concentration and experiment temperature. To our knowledge this is the first study using PMF analysis on AMS chamber data to reveal distinct factors sensitive to temperature.

This analysis demonstrates that α-pinene SOA oxidation level is dependent on both temperature and α-pinene concentration: SOA oxidation level increases with higher temperature and with lower SOA mass loading. The dataset suggests that particles formed at 0 °C are more chemically similar to particles formed at -15 °C than to particles formed at 20 °C. Temperature ramps over a range of 35 °C were only accompanied by slight changes in chemical composition, with increasing oxidation levels during heating ramps and decreasing oxidation levels during cooling-ramps. The investigation demonstrates that the temperature at which particles are formed is decisive for aerosol properties during α-pinene SOA lifetime.

This work confirms that the particle chemical composition is dependent on precursor concentration and particle mass loading. From an atmospheric perspective, it is equally interesting that temperature has a high impact on aerosol chemical composition.

Author contributions

The ACCHA campaign was supervised by MB, ME, MG, and HBP. Experiments were performed by LJ, KK, LLJQ, BR, and RT. The Aerosol Mass Spectrometer (AMS) measurements and AMS data analysis, including Positive Matrix Factorization (PMF) analysis, was carried out by LJ and supervised by MC and MB. LJ prepared the manuscript with contributions from all co-authors.

https://doi.org/10.5194/acp-2020-100
Preprint. Discussion started: 26 February 2020

Atmospheric Chemistry and Physics Discussions

Competing interests

The authors declare that they have no conflict of interest.

Acknowledgements

This work was supported by Aarhus University, The Aarhus University Research Foundation (AUFF), The European Research Council (ERC-Grant nr: 638703-COALA), and the Academy of Finland, Centre of Excellence program (project nr:307331).

References

Abramson, E., Imre, D., Beránek, J., Wilson, J., and Zelenyuk, A.: Experimental determination of chemical diffusion within secondary organic aerosol particles, Phys. Chem. Chem. Phys., 15, 2983-2991, 10.1039/C2CP44013J, 2013.

Aiken, A. C., DeCarlo, P. F., and Jimenez, J. L.: Elemental analysis of organic species with electron ionization high-resolution mass spectrometry, Anal.Chem., 79, 8350-8358, 10.1021/ac071150w, 2007.

Aiken, A. C., Decarlo, P. F., Kroll, J. H., Worsnop, D. R., Huffman, J. A., Docherty, K. S., Ulbrich, I. M., Mohr, C., Kimmel, J. R., Sueper, D., Sun, Y., Zhang, Q., Trimborn, A., Northway, M., Ziemann, P. J., Canagaratna, M. R., Onasch, T. B., Alfarra, M. R., Prevot, A. S. H., Dommen, J., Duplissy, J., Metzger, A., Baltensperger, U., and Jimenez, J. L.: O/C and OM/OC ratios of primary, secondary, and ambient organic aerosols with high-resolution time-of-flight aerosol mass spectrometry, Environ. Sci. Technol., 42, 4478-4485, 10.1021/es703009q, 2008.

Alfarra, M. R.: Insights into the atmospheric organic aerosols using an aerosol mass spectrometer, Thesis, University of Manchester, 2004.

Alfarra, M. R., Coe, H., Allan, J. D., Bower, K. N., Boudries, H., Canagaratna, M. R., Jimenez, J. L., Jayne, J. T., Garforth, A. A., Li, S.-M., and Worsnop, D. R.: Characterization of urban and rural organic particulate in the Lower Fraser Valley using two Aerodyne Aerosol Mass Spectrometers, Atmos. Environ., 38, 5745-5758, 10.1016/j.atmosenv.2004.01.054, 2004.

Axson, J. L., Takahashi, K., De Haan, D. O., and Vaida, V.: Gas-phase water-mediated equilibrium between methylglyoxal and its geminal diol, P. Natl. Acad. Sci. USA, 107, 6687-6692, 10.1073/pnas.0912121107, 2010.

Bahreini, R., Keywood, M. D., Ng, N. L., Varutbangkul, V., Gao, S., Flagan, R. C., Seinfeld, J. H., Worsnop, D. R., and Jimenez, J. L.: Measurements of secondary organic aerosol from oxidation of cycloalkenes, terpenes, and m-xylene using an Aerodyne aerosol mass spectrometer, Environ. Sci. Technol., 39, 5674, 2005.

Canagaratna, M. R., Jayne, J. T., Jimenez, J. L., Allan, J. D., Alfarra, M. R., Zhang, Q., Onasch, T. B., Drewnick, F., Coe, H., Middlebrook, A., Delia, A., Williams, L. R., Trimborn, A. M., Northway, M. J., DeCarlo, P. F., Kolb, C. E., Davidovits, P., and Worsnop, D. R.: Chemical and microphysical characterization of ambient aerosols with the aerodyne aerosol mass spectrometer, Mass Spectrom. Rev., 26, 185-222, 10.1002/mas.20115, 2007.

Canagaratna, M. R., Jimenez, J. L., Kroll, J. H., Chen, Q., Kessler, S. H., Massoli, P., Hildebrandt Ruiz, L., Fortner, E., Williams, L. R., Wilson, K. R., Surratt, J. D., Donahue, N. M., Jayne, J. T., and Worsnop, D. R.: Elemental ratio measurements of organic compounds using aerosol mass spectrometry: characterization, improved calibration, and implications, Atmos. Chem. Phys., 15, 253-272, 10.5194/acp-15-253-2015, 2015.

Cappa, C. D., and Wilson, K. R.: Evolution of organic aerosol mass spectra upon heating: implications for OA phase and partitioning behavior, Atmos. Chem. Phys., 11, 1895-1911, 10.5194/acp-11-1895-2011, 2011.

Chhabra, P. S., Flagan, R. C., and Seinfeld, J. H.: Elemental analysis of chamber organic aerosol using an aerodyne high-resolution aerosol mass spectrometer, Atmos. Chem. Phys., 10, 4111-4131, 10.5194/acp-10-4111-2010, 2010.

Chhabra, P. S., Ng, N. L., Canagaratna, M. R., Corrigan, A. L., Russell, L. M., Worsnop, D. R., Flagan, R. C., and Seinfeld, J. H.: Elemental composition and oxidation of chamber organic aerosol, Atmos. Chem. Phys., 11, 8827-8845, 10.5194/acp-11-8827-2011, 2011.

Craven, J. S., Yee, L. D., Ng, N. L., Canagaratna, M. R., Loza, C. L., Schilling, K. A., Yatavelli, R. L. N., Thornton, J. A., Ziemann, P. J., Flagan, R. C., and Seinfeld, J. H.: Analysis of secondary organic aerosol formation and aging using positive matrix factorization of high-resolution aerosol mass spectra: application to the dodecane low-NOx system, Atmos. Chem. Phys., 12, 11795-11817, 10.5194/acp-12-11795-2012, 2012.

DeCarlo, P. F., Kimmel, J. R., Trimborn, A., Northway, M. J., Jayne, J. T., Aiken, A. C., Gonin, M., Fuhrer, K., Horvath, T., Docherty, K. S., Worsnop, D. R., and Jimenez, J. L.: Field-deployable, high-resolution, time-of-flight aerosol mass spectrometer, Anal. Chem., 78, 8281-8289, 10.1021/ac061249n, 2006.

https://doi.org/10.5194/acp-2020-100
Preprint. Discussion started: 26 February 2020

Atmospheric Chemistry and Physics Discussions

Denjean, C., Formenti, P., Picquet-Varrault, B., Camredon, M., Pangui, E., Zapf, P., Katrib, Y., Giorio, C., Tapparo, A., Temime-Roussel, B., Monod, A., Aumont, B., and Doussin, J. F.: Aging of secondary organic aerosol generated from the ozonolysis of α-pinene: effects of ozone, light and temperature, Atmos. Chem. Phys., 15, 883-897, 10.5194/acp-15-883-2015, 2015a.

Denjean, C., Formenti, P., Picquet-Varrault, B., Pangui, E., Zapf, P., Katrib, Y., Giorio, C., Tapparo, A., Monod, A., Temime-Roussel, B., Decorse, P., Mangeney, C., and Doussin, J. F.: Relating hygroscopicity and optical properties to chemical composition and structure of secondary organic aerosol particles generated from the ozonolysis of α-pinene, Atmos. Chem. Phys., 15, 3339-3358, 10.5194/acp-15-3339-2015, 2015b.

Docherty, K. S., Jaoui, M., Corse, E., Jimenez, J. L., Offenberg, J. H., Lewandowski, M., and Kleindienst, T. E.: Collection Efficiency of the Aerosol Mass Spectrometer for Chamber-Generated Secondary Organic Aerosols, Aerosol Sci. Tech., 47, 294-309, 10.1080/02786826.2012.752572, 2013.

Ehn, M., Thornton, J. A., Kleist, E., Sipilä, M., Junninen, H., Pullinen, I., Springer, M., Rubach, F., Tillmann, R., Lee, B., Lopez-Hilfiker, F., Andres, S., Acir, I.-H., Rissanen, M., Jokinen, T., Schobesberger, S., Kangasluoma, J., Kontkanen, J., Nieminen, T., Kurtén, T., Nielsen, L. B., Jørgensen, S., Kjaergaard, H. G., Canagaratna, M., Maso, M. D., Berndt, T., Petäjä, T., Wahner, A., Kerminen, V.-M., Kulmala, M., Worsnop, D. R., Wildt, J., and Mentel, T. F.: A large source of low-volatility secondary organic aerosol, Nature, 506, 476, 10.1038/nature13032, 2014.

Guenther, A., Hewitt, C. N., Erickson, D., Fall, R., Geron, C., Graedel, T., Harley, P., Klinger, L., Lerdau, M., and McKay, W.: A global model of natural volatile organic compound emissions, J. Geophys. Res.-Atmos., 100, 8873-8892, 1995.

Hakola, H., Tarvainen, V., Laurila, T., Hiltunen, V., Hellén, H., and Keronen, P.: Seasonal variation of VOC concentrations above a boreal coniferous forest, Atmos. Env., 37, 1623-1634, 10.1016/S1352-2310(03)00014-1, 2003.

Hallquist, M., Wenger, J. C., Baltensperger, U., Rudich, Y., Simpson, D., Claeys, M., Dommen, J., Donahue, N. M., George, C., Goldstein, A. H., Hamilton, J. F., Herrmann, H., Hoffmann, T., Iinuma, Y., Jang, M., Jenkin, M. E., Jimenez, J. L., Kiendler-Scharr, A., Maenhaut, W., McFiggans, G., Mentel, T. F., Monod, A., Prévôt, A. S. H., Seinfeld, J. H., Surratt, J. D., Szmigielski, R., and Wildt, J.: The formation, properties and impact of secondary organic aerosol: current and emerging issues, Atmos. Chem. Phys., 9, 5155-5236, 10.5194/acp-9-5155-2009, 2009.

Heald, C. L., Kroll, J. H., Jimenez, J. L., Docherty, K. S., DeCarlo, P. F., Aiken, A. C., Chen, Q., Martin, S. T., Farmer, D. K., and Artaxo, P.: A simplified description of the evolution of organic aerosol composition in the atmosphere, Geophys. Res. Lett., 37, 10.1029/2010GL042737, 2010.

IPCC: Climate Change 2013: The Physical Science Basis. Contribution of Working Group I to the Fifth Assessment Report of the Intergovernmental Panel on Climate Change Cambridge University Press, Cambridge, United Kingdom and New York, NY, USA, 2013.

Jayne, J. T., Leard, D. C., Zhang, X., Davidovits, P., Smith, K. A., Kolb, C. E., and Worsnop, D. R.: Development of an Aerosol Mass Spectrometer for Size and Composition Analysis of Submicron Particles, Aerosol Sci. Tech., 33, 49-70, 10.1080/027868200410840, 2000.

Jenkin, M. E., Shallcross, D. E., and Harvey, J. N.: Development and application of a possible mechanism for the generation of cis-pinic acid from the ozonolysis of α-and β-pinene, Atmos. Env., 34, 2837-2850, 10.1016/S1352-2310(00)00087-X, 2000.

Jimenez, J. L., Canagaratna, M. R., Donahue, N. M., Prevot, A. S. H., Zhang, Q., Kroll, J. H., DeCarlo, P. F., Allan, J. D., Coe, H., Ng, N. L., Aiken, A. C., Docherty, K. S., Ulbrich, I. M., Grieshop, A. P., Robinson, A. L., Duplissy, J., Smith, J. D., Wilson, K. R., Lanz, V. A., Hueglin, C., Sun, Y. L., Tian, J., Laaksonen, A., Raatikainen, T., Rautiainen, J., Vaattovaara, P., Ehn, M., Kulmala, M., Tomlinson, J. M., Collins, D. R., Cubison, M. J., Dunlea, E. J., Huffman, J. A., Onasch, T. B., Alfarra, M. R., Williams, P. I., Bower, K., Kondo, Y., Schneider, J., Drewnick, F., Borrmann, S., Weimer, S., Demerjian, K., Salcedo, D., Cottrell, L., Griffin, R., Takami, A., Miyoshi, T., Hatakeyama, S., Shimono, A., Sun, J. Y., Zhang, Y. M., Dzepina, K., Kimmel, J. R., Sueper, D., Jayne, J. T., Herndon, S. C., Trimborn, A. M., Williams, L. R., Wood, E. C., Middlebrook, A. M., Kolb, C. E., Baltensperger, U., and Worsnop, D. R.: Evolution of Organic Aerosols in the Atmosphere, Science, 326, 1525-1529, 10.1126/science.1180353, 2009.

Kannosto, J., Yli-Pirilä, P., Hao, L.-Q., Leskinen, J., Jokiniemi, J., Mäkelä, J. M., Joutsensaari, J., Laaksonen, A., Worsnop, D. R., and Keskinen, J., Virtanen, A.: Bounce characteristics of α-pinene-derived SOA particles with implications to physical phase, Boreal Environ. Res., 18, 329-340, 2013.

Kirkby, J., Duplissy, J., Sengupta, K., Frege, C., Gordon, H., Williamson, C., Heinritzi, M., Simon, M., Yan, C., Almeida, J., Tröstl, J., Nieminen, T., Ortega, I. K., Wagner, R., Adamov, A., Amorim, A., Bernhammer, A.-K., Bianchi, F., Breitenlechner, M., Brilke, S., Chen, X., Craven, J., Dias, A., Ehrhart, S., Flagan, R. C., Franchin, A., Fuchs, C., Guida, R., Hakala, J., Hoyle, C. R., Jokinen, T., Junninen, H., Kangasluoma, J., Kim, J., Krapf, M., Kürten, A., Laaksonen, A., Lehtipalo, K., Makhmutov, V., Mathot, S., Molteni, U., Onnela, A., Peräkylä, O., Piel, F., Petäjä, T., Praplan, A. P., Pringle, K., Rap, A., Richards, N. A. D., Riipinen, I., Rissanen, M. P., Rondo, L., Sarnela, N., Schobesberger, S., Scott, C. E., Seinfeld, J. H., Sipilä, M., Steiner, G., Stozhkov, Y., Stratmann, F., Tomé, A., Virtanen, A., Vogel, A. L., Wagner, A. C., Wagner, P. E., Weingartner, E., Wimmer, D., Winkler, P. M., Ye, P., Zhang, X., Hansel, A., Dommen, J., Donahue, N. M., Worsnop, D. R., Baltensperger, U., Kulmala, M., Carslaw, K. S., and Curtius, J.: Ion-induced nucleation of pure biogenic particles, Nature, 533, 521, 10.1038/nature17953, 2016.

https://doi.org/10.5194/acp-2020-100
Preprint. Discussion started: 26 February 2020

Kristensen, K., Jensen, L. N., Glasius, M., and Bilde, M.: The effect of sub-zero temperature on the formation and composition of secondary organic aerosol from ozonolysis of alpha-pinene. Environ. Sci.: Processes Impacts, 19, 1220, 10.1039/c7em00231a, 2017.

Kristensen et al. (manuscript submitted to Atmos. Chem. Phys. Discussions. 2020)

Kroll, J. H., and Seinfeld, J. H.: Chemistry of secondary organic aerosol: Formation and evolution of low-volatility organics in the atmosphere, Atmos. Env., 42, 3593-3624, 10.1016/j.atmosenv.2008.01.003, 2008.

Kuwata, M., Zorn, S. R., and Martin, S. T.: Using elemental ratios to predict the density of organic material composed of carbon, hydrogen, and oxygen, Environ. Sci. Technol., 46, 787-794, 2011.

Lanz, V. A., Alfarra, M. R., Baltensperger, U., Buchmann, B., Hueglin, C., and Prévôt, A. S. H.: Source apportionment of submicron organic aerosols at an urban site by factor analytical modelling of aerosol mass spectra, Atmos. Chem. Phys., 7, 1503-1522, 10.5194/acp-7-1503-2007, 2007.

Lee, A. K. Y., Abbatt, J. P. D., Leaitch, W. R., Li, S.-M., Sjostedt, S. J., Wentzell, J. J. B., Liggio, J., and Macdonald, A. M.: Substantial secondary organic aerosol formation in a coniferous forest: observations of both day- and nighttime chemistry, Atmos. Chem. Phys., 16, 6721-6733, 10.5194/acp-16-6721-2016, 2016.

Murphy, B. N., Julin, J., Riipinen, I., and Ekman, A. M. L.: Organic aerosol processing in tropical deep convective clouds: Development of a new model (CRM-ORG) and implications for sources of particle number : PARTICLE NUMBER SOURCES IN CRM-ORG, J. Geophys. Res.-Atmos., 120, 10-10,464, 10.1002/2015JD023551, 2015.

Ng, N. L., Canagaratna, M. R., Zhang, Q., Jimenez, J. L., Tian, J., Ulbrich, I. M., Kroll, J. H., Docherty, K. S., Chhabra, P. S., Bahreini, R., Murphy, S. M., Seinfeld, J. H., Hildebrandt, L., Donahue, N. M., DeCarlo, P. F., Lanz, V. A., Prévôt, A. S. H., Dinar, E., Rudich, Y., and Worsnop, D. R.: Organic aerosol components observed in Northern Hemispheric datasets from Aerosol Mass Spectrometry, Atmos. Chem. Phys., 10, 4625-4641, 10.5194/acp-10-4625-2010, 2010.

Ng, N. L., Canagaratna, M. R., Jimenez, J. L., Chhabra, P. S., Seinfeld, J. H., and Worsnop, D. R.: Changes in organic aerosol composition with aging inferred from aerosol mass spectra, Atmos. Chem. Phys., 11, 6465-6474, 10.5194/acp-11-6465-2011, 2011.

O'Dowd, C. D., Aalto, P., Hmeri, K., Kulmala, M., and Hoffmann, T.: Atmospheric particles from organic vapours, Nature, 416, 497, 10.1038/416497a, 2002.

Pankow, J. F.: An absorption model of gas/particle partitioning of organic compounds in the atmosphere, Atmos. Env., 28, 185-188, 1994a.

Pankow, J. F.: An absorption model of the gas/aerosol partitioning involved in the formation of secondary organic aerosol, Atmos. Env., 28, 189-193, 1994b.

Pathak, R. K., Stanier, C. O., Donahue, N. M., and Pandis, S. N.: Ozonolysis of α-pinene at atmospherically relevant concentrations: Temperature dependence of aerosol mass fractions (yields), J. Geophys. Res.-Atmos., 112, D03201, 10.1029/2006JD007436, 2007.

Paatero, P., and Tapper, U.: Positive matrix factorization: A non - negative factor model with optimal utilization of error estimates of data values, Environmetrics, 5, 111-126, 1994.

Paatero, P.: Least squares formulation of robust non-negative factor analysis, Chemometr. Intell. Lab., 37, 23-35, 10.1016/S0169-7439(96)00044-5, 1997.

Qi, L., Nakao, S., and Cocker, D. R.: Aging of secondary organic aerosol from α-pinene ozonolysis: Roles of hydroxyl and nitrate radicals, J. Air Waste Manage, 62, 1359-1369, 10.1080/10962247.2012.712082, 2012.

Rasmussen, R. A.: What do the hydrocarbons from trees contribute to air pollution?, Journal of the Air Pollution Control Association, 22, 537-543, 1972.

Renbaum-Wolff, L., Grayson, J. W., Bateman, A. P., Kuwata, M., Sellier, M., Murray, B. J., Shilling, J. E., Martin, S. T., and Bertram, A. K.: Viscosity of α-pinene secondary organic material and implications for particle growth and reactivity, P. Natl. Acad. Sci. USA, 110, 8014-8019, 2013.

Riipinen, I., Yli-Juuti, T., Pierce, J. R., Petäjä, T., Worsnop, D. R., Kulmala, M., and Donahue, N. M.: The contribution of organics to atmospheric nanoparticle growth, Nature Geoscience, 5, 453, 10.1038/ngeo1499, 2012.

Shilling, J. E., Chen, Q., King, S. M., Rosenoern, T., Kroll, J. H., Worsnop, D. R., DeCarlo, P. F., Aiken, A. C., Sueper, D., Jimenez, J. L., and Martin, S. T.: Loading-dependent elemental composition of α-pinene SOA particles, Atmos. Chem. Phys., 9, 771-782, 10.5194/acp-9-771-2009, 2009.

Sindelarova, K., Granier, C., Bouarar, I., Guenther, A., Tilmes, S., Stavrakou, T., Müller, J. F., Kuhn, U., Stefani, P., and Knorr, W.: Global data set of biogenic VOC emissions calculated by the MEGAN model over the last 30 years, Atmos. Chem. Phys., 14, 9317-9341, 10.5194/acp-14-9317-2014, 2014.

https://doi.org/10.5194/acp-2020-100
Preprint. Discussion started: 26 February 2020

Atmospheric Chemistry and Physics Discussions

Song, C., Zaveri, R. A., Alexander, M. L., Thornton, J. A., Madronich, S., Ortega, J. V., Zelenyuk, A., Yu, X.-Y., Laskin, A., and Maughan, D. A.: Effect of hydrophobic primary organic aerosols on secondary organic aerosol formation from ozonolysis of α-pinene, Geophys. Res. Lett., 34, L20803, 10.1029/2007GL030720, 2007.

Stanier, C. O., Pathak, R. K., and Pandis, S. N.: Measurements of the volatility of aerosols from alpha-pinene ozonolysis, Environ. Sci. Technol., 41, 2756-2763, 10.1021/es0519280, 2007.

Saathoff, H., Naumann, K. H., Möhler, O., Jonsson, Å. M., Hallquist, M., Kiendler-Scharr, A., Mentel, T. F., Tillmann, R., and Schurath, U.: Temperature dependence of yields of secondary organic aerosols from the ozonolysis of α-pinene and limonene, Atmos. Chem. Phys., 9, 1551-1577, 10.5194/acp-9-1551-2009, 2009.

Topping, D., Connolly, P., and Mcfiggans, G.: Cloud droplet number enhanced by co-condensation of organic vapours, Nature Geoscience, 6, 443, 10.1038/ngeo1809, 2013.

Tröstl, J., Chuang, W. K., Gordon, H., Heinritzi, M., Yan, C., Molteni, U., Ahlm, L., Frege, C., Bianchi, F., Wagner, R., Simon, M., Lehtipalo, K., Williamson, C., Craven, J. S., Duplissy, J., Adamov, A., Almeida, J., Bernhammer, A.-K., Breitenlechner, M., Brilke, S., Dias, A., Ehrhart, S., Flagan, R. C., Franchin, A., Fuchs, C., Guida, R., Gysel, M., Hansel, A., Hoyle, C. R., Jokinen, T., Junninen, H., Kangasluoma, J., Keskinen, H., Kim, J., Krapf, M., Kürten, A., Laaksonen, A., Lawler, M., Leiminger, M., Mathot, S., Möhler, O., Nieminen, T., Onnela, A., Petäjä, T., Piel, F. M., Miettinen, P., Rissanen, M. P., Rondo, L., Sarnela, N., Schobesberger, S., Sengupta, K., Sipilä, M., Smith, J. N., Steiner, G., Tomè, A., Virtanen, A., Wagner, A. C., Weingartner, E., Wimmer, D., Winkler, P. M., Ye, P., Carslaw, K. S., Curtius, J., Dommen, J., Kirkby, J., Kulmala, M., Riipinen, I., Worsnop, D. R., Donahue, N. M., and Baltensperger, U.: The role of low-volatility organic compounds in initial particle growth in the atmosphere, Nature, 533, 527, 10.1038/nature18271, 2016.

Ulbrich, I. M., Canagaratna, M. R., Zhang, Q., Worsnop, D. R., and Jimenez, J. L.: Interpretation of organic components from Positive Matrix Factorization of aerosol mass spectrometric data, Atmos. Chem. Phys., 9, 2891-2918, 10.5194/acp-9-2891-2009, 2009.

Van Krevelen, D. W.: Graphical-statistical method for the study of structure and reaction processes of coal, Fuel, 29, 269-284, 1950.

Virtanen, A., Kannosto, J., Kuuluvainen, H., Arffman, A., Joutsensaari, J., Saukko, E., Hao, L., Yli-Pirilä, P., Tiitta, P., and Holopainen, J.: Bounce behavior of freshly nucleated biogenic secondary organic aerosol particles, Atmos. Chem. Phys., 11, 8759-8766, 10.5194/acpd-11-9313-2011, 2011.

Wang, K., Dickinson, R. E., and Liang, S.: Clear Sky Visibility Has Decreased over Land Globally from 1973 to 2007, Science, 323, 1468-1470, 10.1126/science.1167549, 2009.

Warren, B., Austin, R. L., and Cocker, D. R.: Temperature dependence of secondary organic aerosol, Atmos. Env., 43, 3548-3555, 10.1016/j.atmosenv.2009.04.011, 2009.

WHO: Ambient air pollution: a global assessment of exposure and burden of disease, World Health Organization. Geneva, 2016.

Yatavelli, R. L. N., Mohr, C., Stark, H., Day, D. A., Thompson, S. L., Lopez‐Hilfiker, F. D., Campuzano‐Jost, P., Palm, B. B., Vogel, A. L., Hoffmann, T., Heikkinen, L., Äijälä, M., Ng, N. L., Kimmel, J. R., Canagaratna, M. R., Ehn, M., Junninen, H., Cubison, M. J., Petäjä, T., Kulmala, M., Jayne, J. T., Worsnop, D. R., and Jimenez, J. L.: Estimating the contribution of organic acids to northern hemispheric continental organic aerosol, Geophys. Res. Lett., 42, 6084-6090, 10.1002/2015GL064650, 2015.

Zhang, Q., Jimenez, J. L., Canagaratna, M. R., Allan, J. D., Coe, H., Ulbrich, I., Alfarra, M. R., Takami, A., Middlebrook, A. M., Sun, Y. L., Dzepina, K., Dunlea, E., Docherty, K., DeCarlo, P. F., Salcedo, D., Onasch, T., Jayne, J. T., Miyoshi, T., Shimono, A., Hatakeyama, S., Takegawa, N., Kondo, Y., Schneider, J., Drewnick, F., Borrmann, S., Weimer, S., Demerjian, K., Williams, P., Bower, K., Bahreini, R., Cottrell, L., Griffin, R. J., Rautiainen, J., Sun, J. Y., Zhang, Y. M., and Worsnop, D. R.: Ubiquity and dominance of oxygenated species in organic aerosols in anthropogenically-influenced Northern Hemisphere midlatitudes, Geophys. Res. Lett., 34, L13801-n/a, 10.1029/2007GL029979, 2007.

Zhang, X., McVay, R. C., Huang, D. D., Dalleska, N. F., Aumont, B., Flagan, R. C., and Seinfeld, J. H.: Formation and evolution of molecular products in α-pinene secondary organic aerosol, P. Natl. Acad. Sci. USA, 112, 14168-14173, 10.1073/pnas.1517742112, 2015.

https://doi.org/10.5194/acp-2020-100
Preprint. Discussion started: 26 February 2020

Atmospheric Chemistry and Physics Discussions

Table 1. Overview of experimental details for the ACCHA experiments included in this work. The experiments are constant temperature (const. temp.) experiments and/or temperature ramp (temp. ramp) experiments.

Exp. #	Exp. ID	Exp. type	O_3	α-pinene	Temp. avg. at const. temp. (±std. dev.)*	RH avg. at const. temp. (±std. dev.) [start to end]*	Ramp start-to-end temp	Ramp start-to-end RH	Density
			ppb	ppb	°C	%	°C	%	g cm^{-3}
1.1	20161202	Const. temp (20 °C)	104	10	20.2 (±0.0)	0.5 (±0.7) [0.0-2.1]			1.25
1.2	20161208	Const. temp (0 °C)	105	10	0.0 (±0.2)	6.0 (±2.9) [2.8-12.7]			1.20
1.3	20161207	Const. temp (-15 °C)	106	10	-15.1 (±0.3)	10.3 (±2.1) [8.0-15.0]			1.16
1.4	20161209	Temp. ramp (20 to -15 °C)	103	10			19.8 to -12.0	Na	1.23
1.5	20161220	Temp. ramp (-15 to 20 °C)	113	10			-14.0 to 19.6	11.7 to 1.7	1.17
2.1	20161212	Const. temp (20 °C) + temp. ramp (20 to -15 °C)	105	50	20.0 (±0.2)	0.8 (±0.9) [0.0-3.0]	20.2 to -12.4	4.3 to 79.5	1.23
2.2	20161219	Const. temp (0 °C) + temp. ramp (0 to -15 to 20 °C)	107	50	-0.3[A] (±0.1)	7.0[A] (±0.2) [6.9-7.5]	~0 to -13.2 to 18.6	~21 to 52.0 to 7.3	1.15
2.3	20161221	Const. temp (-15 °C) + temp. ramp (-15 to 20 °C)	113	50	-15.0 (±0.2)	24.7 (±3.6) [19.3-31.7]	-15.1 to 18.6	33.0 to7.3	1.12
3.1	20170112	Const. temp (20 °C)	100	50	20.0 (±0.2)	1.7 (±1.6) [0.0-4.6]			1.21
3.2	20170116	Const. temp (0 °C)	105	50	0.0[B] (±0.1)	8.9[B] (±0.1) [8.6-9.1]			1.14
3.3	20170113	Const. temp (-15 °C)	105	50	-15.4 (±0.6)	14.5 (±3.8) [11.1-23.0]			1.13

[A]Temperature and relative humidity probe failure after 59 minutes and the rest of the constant temperature experiment and in the very beginning of the ramp; [B]temperature and relative humidity probe failure after 42 minutes; *averages of temperature and relative humidity are based on data from the time of α-pinene injection to filter sampling and might differ slightly from the values reported in Kristensen et al. (submitted manuscript). Densities are 30 minutes averages obtained by the end of the experiments (1.1-1.5 and 3.1-3.3) or the constant temperature experiments (2.1-2.3).

Table 2. Characteristics of the four factors obtained from PMF analysis of experiments (1.1, 1.2, 1.3, 1.4, 1.5, 3.1, 3.2, and 3.3) according to Figure 2. For each factor the fraction of m/z 43 (f_{43}) and m/z 44 (f_{44}) relative to the total mass spectra are stated in percent.

Factor	Dominating appearance	Characteristics	f_{43}	f_{44}	O:C ratio	H:C ratio
Factor 1 (temperature)	High temperature	Fraction decrease with decreasing temperature at both α-pinene concentrations.	14	9	0.56	1.65
Factor 2 (concentration/loading)	50 ppb (high) α-pinene concentration, high particle mass loading	High fraction in all 50 ppb experiments. Appears only slightly in 10 ppb experiments.	10	3	0.26	1.60
Factor 3 (concentration/loading)	10 ppb (low) α-pinene concentration, low particle mass loading	High fraction in all 10 ppb experiments. Almost nonexistent in 50 ppb experiments.	7	8	0.39	1.59
Factor 4 (temperature)	Low temperature	Fraction decrease with increasing temperature at both α-pinene concentrations.	13	4	0.34	1.71

https://doi.org/10.5194/acp-2020-100
Preprint. Discussion started: 26 February 2020

Atmospheric Chemistry and Physics Discussions

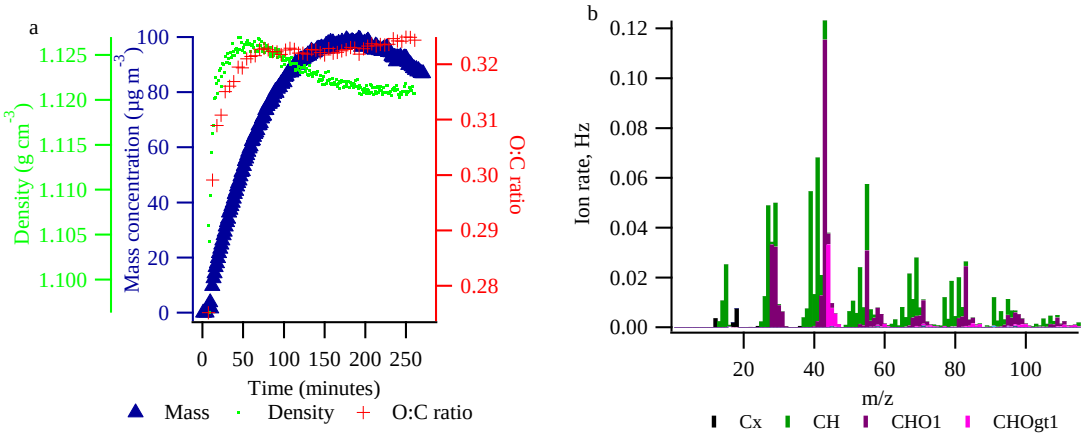

Figure 1. (a) Evolution of SOA mass (density corrected), density, and O:C ratio during a typical experiment (50 ppb α-pinene, -15 °C, experiment 2.3) and (b) mass spectra of the experiment obtained at mass peak (5 minutes average). gt means greater than.

https://doi.org/10.5194/acp-2020-100
Preprint. Discussion started: 26 February 2020

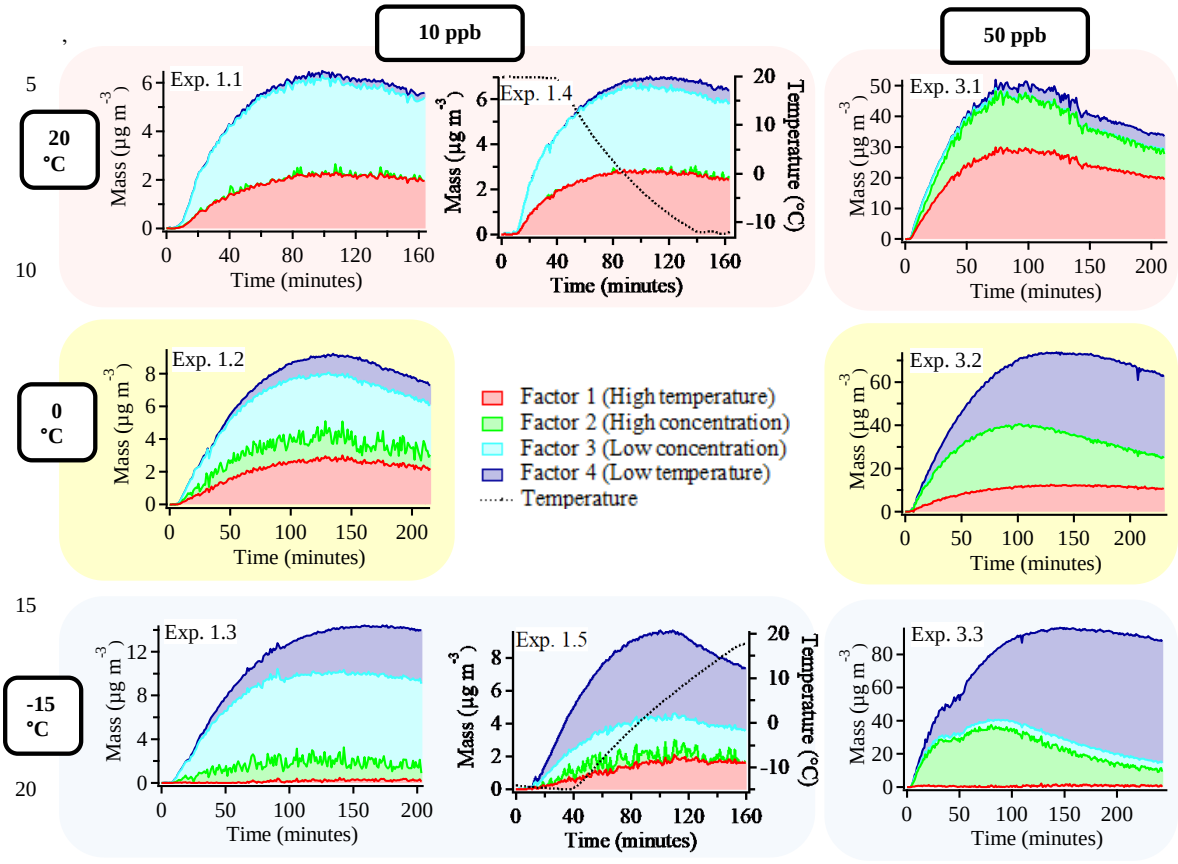

Figure 2. Mass evolution (µg m^{-3}) (y-axis) of the four factors from PMF analysis of the combined AMS data set including experiments with an initial α-pinene concentration of 10 ppb and 50 ppb respectively, at constant temperatures of 20 °C (experiments 1.1 and 3.1), 0 °C (experiments 1.2 and 3.2), and -15 °C (experiments 1.3 and 3.3) and at 10 ppb initial α-pinene concentration in the temperature ramp experiments from 20 °C to -15 °C (experiment 1.4) and -15 °C to 20 °C (experiment 1.5). 10 ppb experiments are shown in the left and middle column of graphs while each row of graphs represent different initial temperatures.

https://doi.org/10.5194/acp-2020-100
Preprint. Discussion started: 26 February 2020

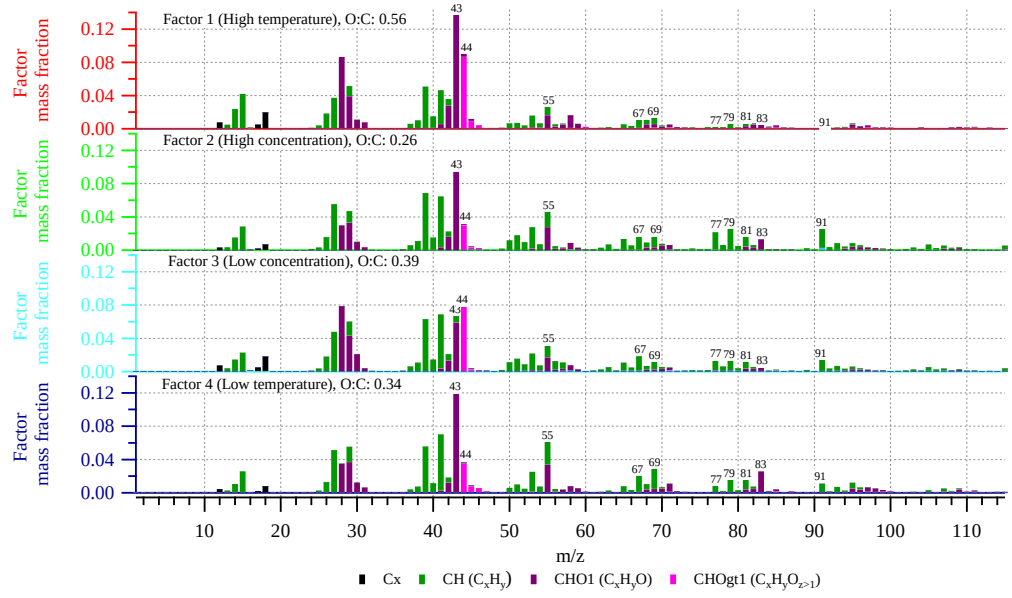

Figure 3. Mass spectra of the four factors from the PMF analysis (see also Figure 2 and Table 2). gt means greater than.

https://doi.org/10.5194/acp-2020-100
Preprint. Discussion started: 26 February 2020

Atmospheric Chemistry and Physics Discussions

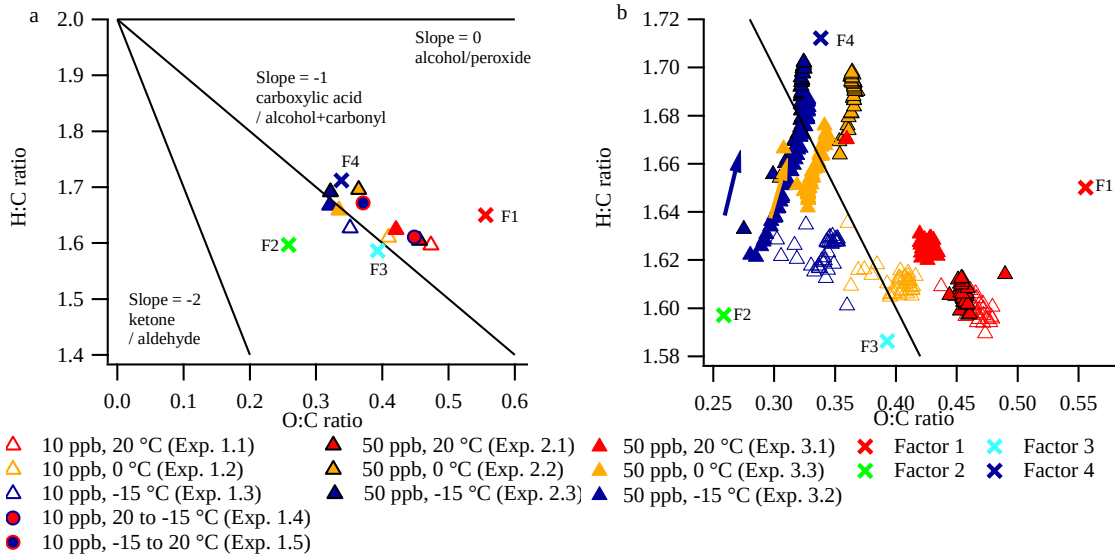

Figure 4. Van Krevelen plots (H:C ratio vs. O:C ratio) (a) at SOA mass peak (five data point average) and (b) during the constant temperature experiments in this work (~5 minutes time resolution, arrows indicate direction of time). The lines in the Van Krevelen plot are based on Heald et al. (2010) and Ng et al. (2011). The positions of the four factors obtained from the PMF analysis are indicated by crosses: F1: Factor 1 (high temperature), F2: factor 2 (high concentration), F3: Factor 3 (low concentration), and F4: Factor 4 (low temperature).

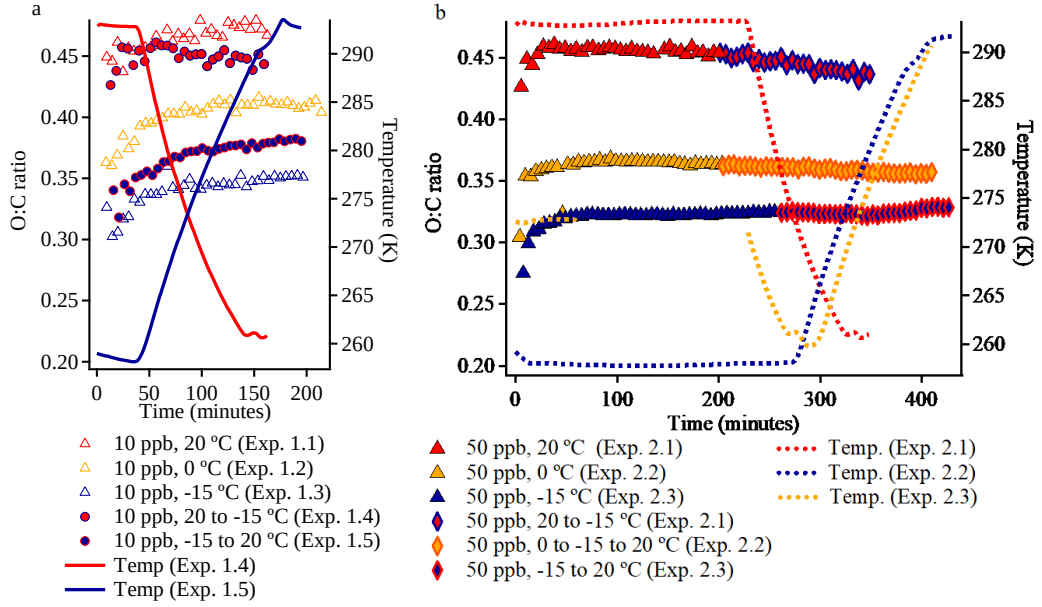

Figure 5. Time series of O:C ratio in (a) 10 ppb α-pinene experiments (1.1-1.5) and (b) 50 ppb α-pinene experiments (2.1-2.3).

https://doi.org/10.5194/acp-2020-100
Preprint. Discussion started: 26 February 2020

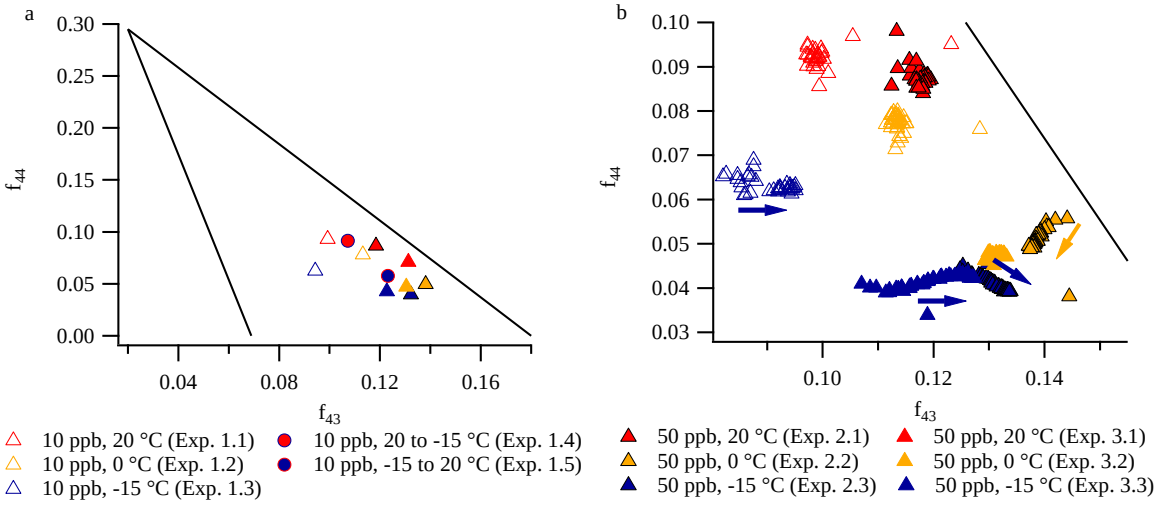

Figure 6. The elemental composition of particles formed in experiments 1.1-1.3, 2.1-2.3, and 3.1-3.3 depicted in triangle plots (f_{44} vs. f_{43}) (a) at mass peak (five data point average) and (b) during the experiments (~5 minutes time resolution, arrows indicates direction of time). In the triangle plots the lines ($y = -6.0204x + 0.4154$ and $y = -1.8438x+0.3319$, where $0.069 \leq x \leq 0.18$ and $y \leq 0.295$) define the common composition of oxygenated organic aerosol (Ng et al., 2010).

https://doi.org/10.5194/acp-2020-100
Preprint. Discussion started: 26 February 2020

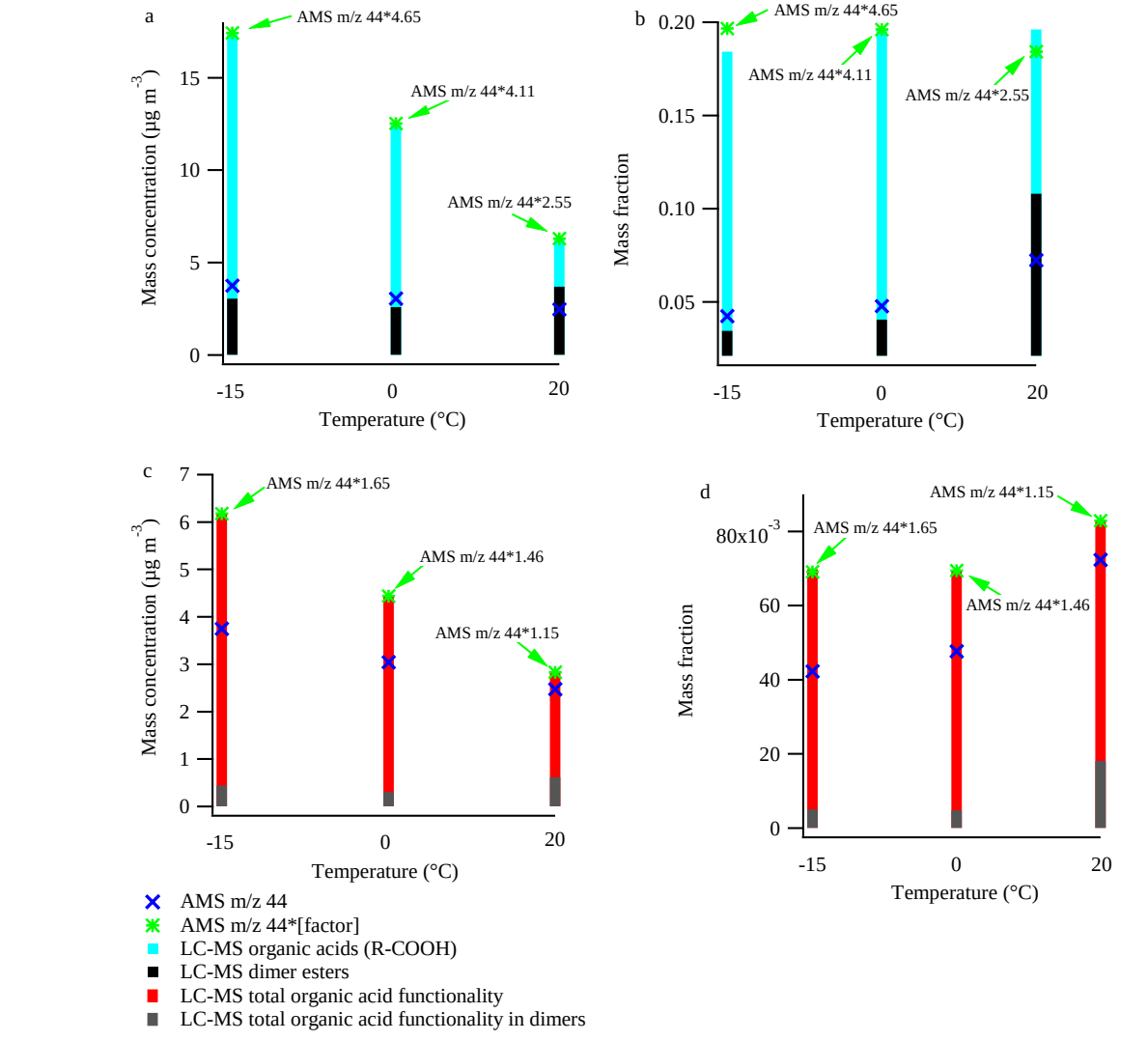

Figure 7. LC-MS derived organic acid (R-COOH) mass concentration (panel a) and organic acid mass fraction (panel b) at -15, 0, and 20 °C. The organic acid functionality (-COOH) mass concentration and mass concentration at the three temperatures are shown in panels c and d respectively. Additionally the corresponding results related to dimers are shown. The panels also show m/z 44 - a tracer of organic acids - from the AMS mass spectra and the scaling factors to be applied to reach the level of organic acid (functionality) measured by the LC-MS. The particle filter samples analyzed by the LC-MS are obtained by the end of the experiments (see Table 1) while the AMS results are obtained right before the filter sampling, 10 minutes average). The figure is based on data from experiments 3.1-3.3.